Proceedings of Ninth World Conference on Earthquake Engineering
August 2-9, 1988, Tokyo-Kyoto, JAPAN (Vol.IV)

6-6-3

CORRELATION OF BOND AND SHEAR IN RC BEAM-COLUMN CONNECTIONS SUBJECTED TO SEISMIC FORCES

Hiroshi NOGUCHI[1] and Kohichiro KURUSU[2]

[1]Department of Architectural Engineering, Chiba University, Chiba, Japan
[2]Ohbayashi-Gumi Corporation, Osaka, Japan

SUMMARY

Eight half-scale reinforced concrete interior beam-column joints were tested to assess the interrelation between the bond situation of beam longitudinal reinforcing bars passing through a joint and joint shear stress level which are important factors for the aseismic design of beam-column joints. The effect of the bond situation of beam bars on the role of joint shear reinforcement was also discussed from the test results.

INTRODUCTION

With the rationalization in the design, it has been required to ensure the shear strength and ductility of the structural member, such as beams and columns. The high strength and large-sized deformed bar was developed, and the dimensions of sections in beams and columns have gotten smaller. Consequently the increased ultimate strength of beams and columns yields the high stress state in the beam-column joint. The weak point in the RC frame is going to shift from the constituent members to the joint. Under these present situation, it is considered to be probable that the joint fails in shear under reversed cyclic loading after the flexural yielding of beams, and the development of the rational design method for the beam-column joint has become a matter of concern in Japan. The development length of beam bars passing through a joint and the limitation to the joint shear stress are considered to be very important in the design. In this study, the correlation between the bond situation of beam bars passing through a joint and joint shear stress level are discussed for the experimental results.

BOND INDEXES

Bond index, τ_s, which was defined in Eq. (1), was used for the quantitative expression of the bond characteristics of beam longitudinal bars passing through a joint.

$$\tau_s = {}_s\sigma_y A_s / \phi / h_c \ (\mathrm{MPa}) \qquad (1)$$

in which ${}_s\sigma_y$ = yielding strength of beam bars, A_s = nominal sectional area of beam bars, ϕ = nominal perimeter of beam bars and h_c = column depth. In this test, deformed bars of D10 (nominal diameter = 10 mm) with the low yield strength were used for the specimens with good bond, and τ_s = 5.0 MPa. Deformed bars of D13 (nominal diameter = 13 mm) with high yield strength were used for the

specimens with poor bond, and τ_s = 7.45 - 8.04 MPa.

ULTIMATE JOINT SHEAR STRESS

The ultimate joint shear stress-area ratio of joint reinforcement relationships are shown in Fig. 1. The recent experimental data were plotted in Fig. 1 including the specimens in this test in addition to the original figure by Ogura et al.(Ref.1), and p_w = area ratio of joint reinforcement = a_w / (column depth x beam effective depth x 7/8), a_w = area of joint reinforcement, F_c =compressive strength of concrete, MPa, V_j = effective joint volume = (column effective depth x 7/8) x (beam effective depth x 7/8) x ((column width + beam width) / 2). From the previous test results in Fig. 1, it was shown that joints failed in shear after the beam flexural yielding for $0.30 \leqq \tau_{pu}/F_c \leqq 0.33$ for $0.03 \leqq p_{ws}\sigma_y/F_c \leqq 0.35$, and joints did not fail in shear for $\tau_{pu}/F_c \leqq 0.28$. Little difference in τ_{pu}/F_c according to $p_{ws}\sigma_y/F_c$ was observed. In this test, the joint shear stress level was varied in the region of the resrtricted value in ACI-ASCE 352 Recommendations. (Ref.2)

TEST SPECIMENS

Eight half-scale RC interior beam-column joints (called CC-series), removed from a plane frame and columns at arbitrarily assumed inflection points, were tested to study the effects of joint shear stress level and the bond situation of beam bars passing through a joint on the ultimate strength of the joint and the failure mode. The dimensions of members were common in the eight specimens; beams were 200x300 mm, and columns were 300x300 mm, as shown in Fig. 2. The specimens were all designed to develop weak-beam strong-column behaviour.

Specimens in Series 1 were provided with only one set of D6 as the joint shear reinforcement to observe the behaviour of the joint with a smaller amount of shear reinforcement, p_w = 0.1 %, as shown in Table 1. The beam longitudinal reinforcement was chosen to be smaller-sized, D10 with the lower yield strength (SD24 equivalent) for specimens NO.1 and NO.2 so that the bond situation would be improved in the beam longitudinal reinforcing bars. The beam longitudinal reinforcement was chosen to be larger-sized, D13 with the higher yield strength (SD30) for specimens NO.3 and NO.4 so that the bond deterioration would be observed in the beam longitudinal reinforcing bars. The joint shear stress level was selected in the region of τ_{pu}/F_c = 0.27 so that the failure mode would change from the beam flexural failure without joint shear failure to the joint shear failure after developing flexural yielding at the ends of connecting beams.

Specimens in Series 2 were provided with the joint shear reinforcing bars according to 1/2 x $p_{ws}\sigma_y$ so that half of the entire shear could be resisted by the shear reinforcement. From Kitayama and Otani's C-series test (Ref.4), it was pointed out that the amount of the joint shear reinforcement could be reduced to one half even the structure was expected to deform at a story drift angle of 1/23 rad. As the joint shear failure occurred for the specimens in Series 1, the joint shear stress level was reduced in Series 2. Material properties are shown in Table 2.

TESTING METHOD

The specimens were tested in upright position as shown in Fig. 3. The column ends were supported by a horizontal roller and a mechanical hinge. The constant vertical load (axial stress, σ_o = 1.96 MPa) was loaded at the top of t column by 30 tonf (294 KN) actuator, and reversing loads were applied to the b

ends by two acutuators of 100 tonf (981 KN) capacity. The forced story drift history of the two series of tests is shown in Fig. 4. The deformations of beams and columns relative to the beam-column joints, joint shear deformation, beam end rotation and slips of beam longitudinal reinforcement were measured by strain-gauge type displacement transducers. The strain distribution of beam longitudinal reinforcement and that of joint shear reinforcing bars were measured by a series of strain gauges. The loads applied to the beam ends by the actuator were measured by load cells. Crack pattern and the process to failure were observed, and crack widths in a joint were measured by the crack scale.

TEST RESULTS

There was no remarkable difference in the various experimental phenomena between specimens in which only the joint shear stress levels were different. Therefore, the test results on four specimens NO.2, NO.4, NO.5, NO.7 in which the joint shear stress levels were nearly equal were mainly discussed in this paper.

Crack Patterns The crack patterns observed at the end of loading are shown in Fig. 5. For specimens in Series 1, the shear crack width increased at the center of a joint during loading at a story drift angle of 1/53 rad after the beam flexural yielding. The shell concrete of a joint swelled out slightly at a story drift angle of 1/53 rad. Crushed concrete spalled off from the bottom of beams in the plastic hinge zones during the sixth and seventh cyclic loadings to a story drift angle of 1/53 and 1/26 rad, respectively. For the specimens of Series 2 in which a joint was reinforced so that half of the entire shear could be resisted by the shear reinforcement, the joint shear cracks did not widen. Flexural cracks developed at the critical section of a beam at a story drift angle of 1/53 rad, and plastic hinge regions of a beam spread gradually.

Story Shear-Story Drift Relations The envelope curves of the story shear-story drift relations are shown in Fig. 6 for specimens NO.2, NO.4, NO.5 and NO.7. The shape of the envelope curve for specimen NO.5 with heavier joint shear reinforcement and improved bond characteristics for the beam bars was smooth in the first and third quadrants in Fig. 6, because there was no strength decay during the load cycles with the same maximum story drift. But the shape of the envelope curve for the other three specimens with a small amount of joint shear reinforcement or deteriorative bond characteristics for beam bars was like the teeth of a saw because of the strength decay. In the second and fourth quadrants in Fig. 6, specimen NO.5 showed a fat spindle shaped hysteretic behaviour, but the other specimens showed typical pinched effects.

Joint Shear Stress-Shear Distortion Relations Joint shear stress-shear distortion relations are shown in Fig. 7 for specimens NO.2, NO.4, NO.5 and NO.7. Shear yielding was developed at the fifth load cycle to a drift angle of 1/53 for specimens NO.2 and NO.4 with a small amount of joint shear reinforcement. Thereafter, joint shear distortion gradually increased to the value of 20×10^{-3} rad at the ninth load cycle to a drift angle of 1/18, and the failure mode was joint shear failure. Joint distortion was rather small ($\gamma \leq 4\times10^{-3}$ rad) in specimens NO.5 and NO.7 with heavier shear reinforcement, and the failure mode was beam flexural failure without joint shear failure. Comparing the relations of specimens NO.2, NO.4, NO.5 and NO.7, a large amount of joint shear reinforcement (p_w = 1.15%) *was obviously effective on the control of the shear strength decay* and shear deformation in the joint.

Deflection Components of Story Drift The contribution of parts of a specimen to the story drift is shown in Fig. 8. For specimens NO.2 and NO.4 with a small amount of joint shear reinforcement, the deflection of a joint gradually increased and contributed about 30 % to the total story drift. For specimens NO.5

and NO.7 with heavier joint shear reinforcement, the deflection of a joint was limited within 5 % to the total story drift.

Strains in Joint Shear Reinforcement The measured strains in all joint shear reinforcement were plotted in Fig. 9 from the seventh to ninth load cycle (story drift angles of 1/23 - 1/18). Note that the strains in the joint shear reinforcement remarkably increased in specimen NO.5, but they even decreased in specimen NO.7, because of the strength decay during loading with the same maximum story drift.

CONCLUDING REMARKS

1) When the amount of joint shear reinforcement was small (p_w=0.1 %), the joint shear failure occurred at the story drift angle of 1/53 after beam flexural yielding even under the maximum joint shear stresses, $0.23 \leq \tau_{pu}/F_c \leq 0.28$, which were less than the limited value in ACI-ASCE 352 Recommendations. (Ref.2) The hysteretic loop of the story shear-story drift relations showed a contra-S-shape during loading to the story drift of 1/53.

2) When a joint was reinforced so that half of the entire shear could be resisted by the shear reinforcement, the joint shear distortion was restrained to 4×10^{-3} rad, and the joint failure was prevented effectively up to a story drift angle of 1/18 rad after beam flexural yielding. The specimens with good bond characteristics for beam bars showed a fat spindle shape, but the specimens with bond deteriorative characteristics for beam bars showed a contra-S-shape during loading to a story drift angle of 1/53.

3) The joint shear reinforcement had the effects of restraining the shear deterioration caused by the increase of the joint shear distortion and preventing the potential joint shear strength decay.

4) When the amount of joint shear reinforcement was larger, the strains in specimen with good bond characteristics for beam bars was remarkably larger than that in specimen with bond deteriorative characteristics during loading to a story drift angle of 1/26.

ACKNOWLEDGMENTS

Support of this work was provided by the Ministry of Education, Science and Culture under the Project No. 60550388 in Grant-in-Aid for Scientific Research (C). The authors wish to express their sincere gratitude to Professor H. Aoyama at the University of Tokyo for his guidance and encouragement.

REFERENCES

1. Ogura, K. and Sekine, M., "The State of the Art of the Studies on the Reinforced Concrete Beam to Column Joint," Concrete Journal, Vol.19, No.9, 2-15, Sept. 1981 (in Japanese).
2. ACI-ASCE Committee 352, "Recommendations for Design of Beam-Column Joints in Monolithic Reinforced Concrete Structures," ACI Journal, V.82, No.3, 226-283, May-June 1985.
3. Standards Association of New Zealand, "Code of Practice for the Design of Concrete Structures," NZS 3101. Wellington, 1982.
4. Kitayama, K., Kurusu, K., Otani, S. and Aoyama, H., "Behaviour of Beam-Column Connections with Improved Beam Reinforcement Bond," Trans. of JCI, Vol.7, 551-558, 1984.

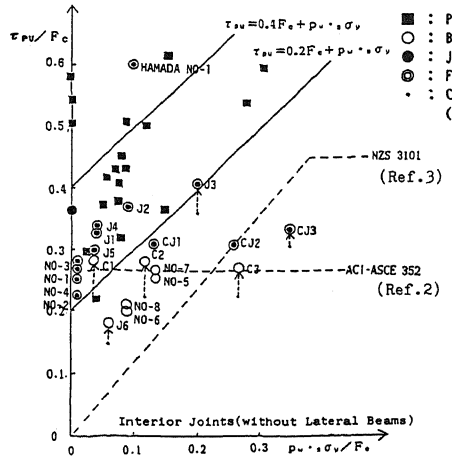

Fig. 1 Ultimate Joint Shear Stress-Joint Reinforcement Ratio Relations

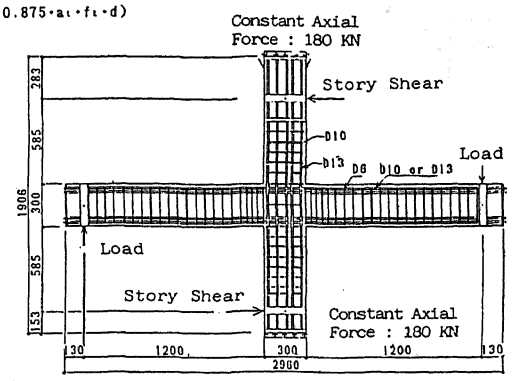

Fig. 2 Reinforcement Details of Specimen (Series 1)

Table 1: Properties of Specimens

	First Series				Second Series			
Specimen	NO.1	NO.2	NO.3	NO.4	NO.5	NO.6	NO.7	NO.8
Beam								
Top Bars	12-D10	10-D10	6-D13	5-D13	10-D10	8-D10	5-D13	4-D13
Bottom Bars	12-D10	10-D10	6-D13	5-D13	10-D10	8-D10	5-D13	4-D13
P_t(%)	1.67	1.39	1.49	1.25	1.39	1.11	1.25	1.00
Stirraps	2-D6	2-D6	2-D6	2-D6	2-D6	2-D6	2-D6	2-D6
Column								
Total Bars	18-D13	16-D13	18-D13	16-D13	16-D13	12-D13	16-D13	12-D13
P_g(%)	2.61	2.31	2.61	2.31	2.31	1.72	2.31	1.72
Hoops	2-D10	2-D10	2-D10	2-D10	2-D10	2-D10	2-D10	2-D10
Connection								
Hoops	2-D6	2-D6	2-D6	2-D6	24-D6	16-D6	24-D6	16-D6
P_w(%)	0.10	0.10	0.10	0.10	1.15	0.76	1.15	0.76

Table 2: Material Properties of Test Specimens

	Steel σ_y(MPa)				Concrete		
	Beam		Column	Joint	F_c (MPa)	f_c (MPa)	Slump (cm)
First Series	D10	D13	D13	D6	34.1	2.35	10.3
	325	388	354	354			
Second Series	D10	D13	D13	D6	29.3	2.16	20.5
	325	374	374	322			

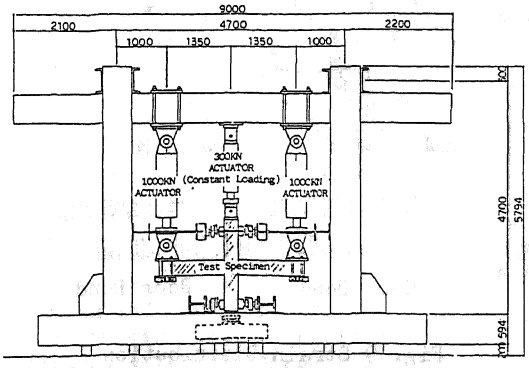

Fig. 3 Test Specimen in Loading Setup

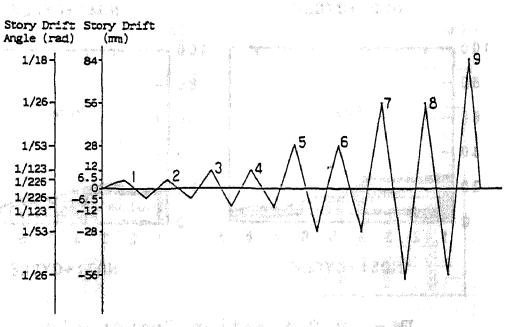

Fig. 4 Loading History

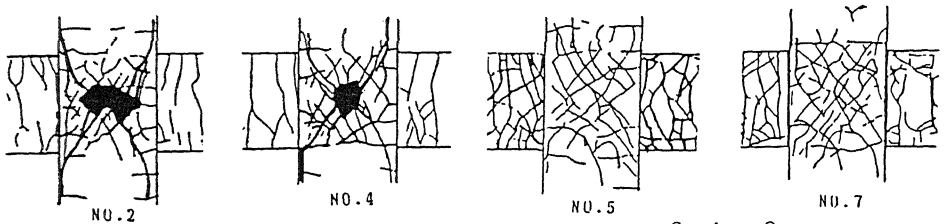

Fig. 5: Crack Patterns after Test

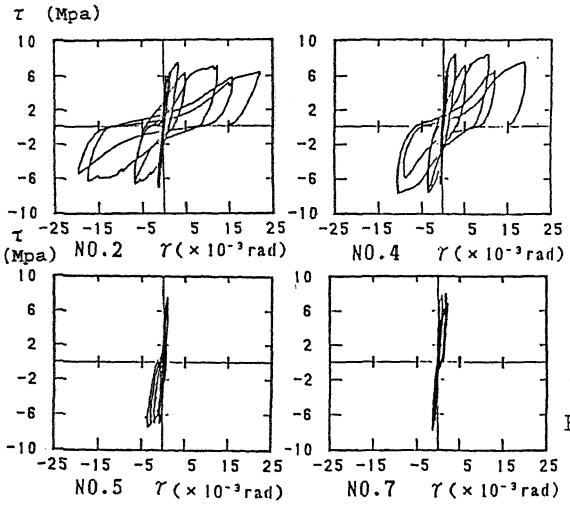

Fig. 7 Joint Shear Stress-Shear Distortion Relations

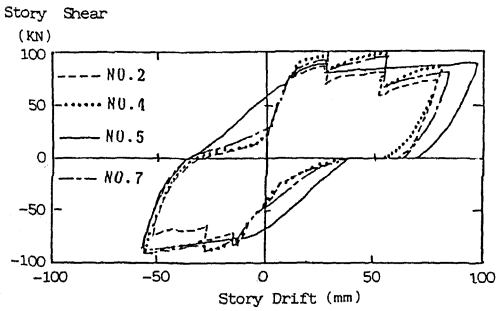

Fig. 6 Envelope Curves of Story Shear-Story Drift Relations

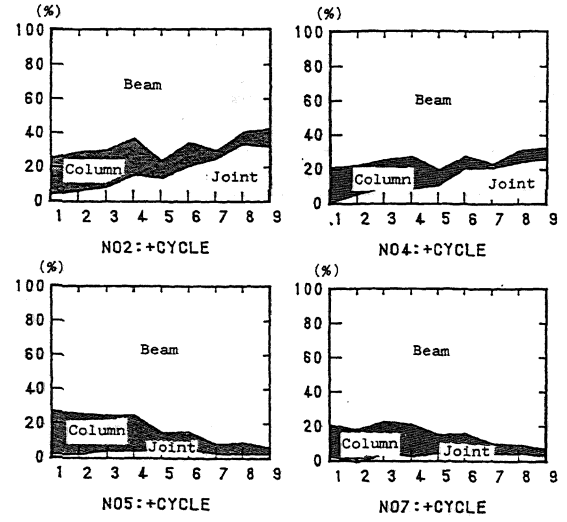

Fig. 8 Deflection Components of Story Drift

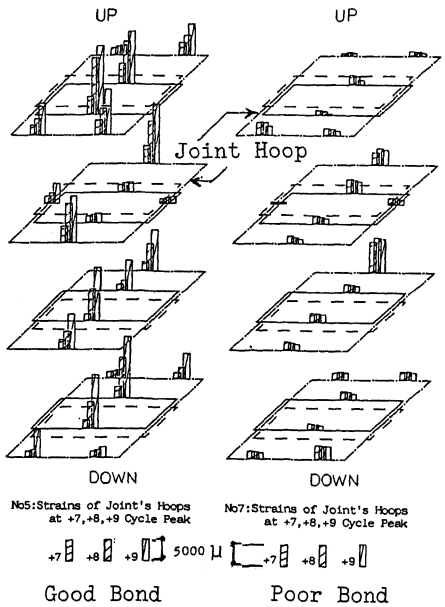

Fig. 9 Strain Distribution in Joint Shear Reinforcement